Polymer 50 (2009) 4696–4705

Contents lists available at ScienceDirect

Polymer

journal homepage: www.elsevier.com/locate/polymer

Elastic misfit in two-phase polymer

R.R. Mocellini [a], O.A. Lambri [a,b,*], C.L. Matteo [c,d], J.A. García [e], G.I. Zelada-Lambri [a], P.A. Sorichetti [c], F. Plazaola [f], A. Rodríguez-Garraza [g], F.A. Sánchez [h]

[a] Facultad de Ciencias Exactas, Ingeniería y Agrimensura, Universidad Nacional de Rosario, Laboratorio de Materiales, Escuela de Ingeniería Eléctrica, Avda. Pellegrini 250, 2000 Rosario, Argentina
[b] Instituto de Física Rosario – Consejo Nacional de Investigaciones Científicas y Técnicas (CONICET), Argentina
[c] Departamento de Física, Facultad de Ingeniería, Universidad de Buenos Aires, Avda. Paseo Colón 850, 1063 Buenos Aires, Argentina
[d] Consejo Nacional de Investigaciones Científicas y Técnicas (CONICET), Argentina
[e] Departamento de Física Aplicada II, Facultad de Ciencias y Tecnología, Universidad del País Vasco, Apdo. 644, 48080 Bilbao, País Vasco, Spain
[f] Elektrika eta Elektronika Saila, Zientzia eta Teknologia Fakultatea, Euskal Herriko Unibertsitatea, P.K. 644, 48080 Bilbao, Spain
[g] Departamento de Física, Facultad de Ciencias, Universidad de Buenos Aires, Argentina
[h] División Física de Reactores Avanzados, Reactor Nuclear RA6, Centro Atómico Bariloche, Comisión Nacional de Energía Atómica, Río Negro, Argentina

ARTICLE INFO

Article history:
Received 5 March 2009
Received in revised form
19 July 2009
Accepted 22 July 2009
Available online 26 July 2009

Keywords:
EPDM
Mechanical behaviour
Chemi-crystallization

ABSTRACT

The present work presents a model to evaluate the average inclusion strain in the matrix of a bulk polymer. The new model considers a two-phase polymer (matrix and inclusions), where the bulk sample is partitioned in small elementary cubes. Taking a large enough number of partitions, each element can be considered to be composed of a single phase, where adjacent elements may be composed by different phases. Moreover, the size of the elementary cubes of the partition is chosen to allow for the accurate representation of the material properties. The model takes into account the interaction between inclusions, and therefore, for different amount of volume fractions of inclusions within the matrix. Experimental results show that the model gives an accurate representation of the average strain in the rubber matrix caused by the crystallites in a two-phase polymer as EPDM (ethylene–propylene-diene M-class rubber).

1. Introduction

Semi-crystalline polymers are composed by two phases, where the crystalline zones, called also crystallites, are embedded into an amorphous matrix [1,2]. From a mesoscopical point of view, crystallites can be considered as inclusions into an elastic matrix. In the theory of elasticity one inclusion is a region where its shape is different from the surrounding bulk matrix or where the elastic constant are different from the bulk matrix. The problem of inclusion in solids has been largely studied in the literature in several works [3–9]. For instance, Lee et al. [8] studied the elasto-plastic behaviour in a matrix originated by an isolated inclusion, assuming ideal plastic behaviour for an isotropic matrix. In their study the case of purely elastic accommodation of stress and strain related to a misfitting spherical precipitate was discussed in the first place.

On the other hand, Takayanagi [1,10] on his model introduces a partition of the polymer in elements of prismatic shape in order to describe the relaxation processes in a two-phase polymer. In Takayanagi's model the crystalline and amorphous regions were in series, so that each one is subjected to the same stress and their compliances are added like in the Reuss approximation [1,10].

In the present work, the basic ideas for the purely elastic treatment stated in the paper by Lee et al. will be used together with the Takayanagi work for describing the average inclusion strain in the bulk matrix of a two-phase polymer, as the ethylene–propylene-diene M-class rubber, EPDM. However, the model developed in the present work is a more general, allowing for the interaction between inclusions, and therefore for different amount of volume fractions of inclusions within the matrix. In fact, the new model presented here considers a two-phase polymer where the bulk sample is partitioned in small elementary cubes. Taking a large enough number of partitions, each element can be considered as composed by one of the two different phases. Moreover, the size of the elementary cubes of the partition is chosen in order to allow the accurate representation of the material properties. This representation was recently used by Mocellini et al., for the study of mechanical and electrical relaxation processes in two-phase polymers [11,12].

* Corresponding author at: Instituto de Física Rosario, Facultad de Ciencias Exactas, Ingeniería y Agrimensura, Universidad Nacional de Rosario - CONICET, Laboratorio de Materiales, Escuela de Ingeniería Eléctrica, Avda. Pellegrini 250, 2000 Rosario, Argentina. Fax: +54 0341 480 2654/482 17 72.
E-mail address: olambri@fceia.unr.edu.ar (O.A. Lambri).

0032-3861/$ – see front matter © 2009 Elsevier Ltd. All rights reserved.
doi:10.1016/j.polymer.2009.07.037

Finally, the model will be successfully verified through experimental studies using dynamic mechanical analysis and dielectric relaxation techniques applied to EPDM with both, different crystalline volume fraction and size of crystallites promoted by neutron irradiation. Neutron irradiation on EPDM leads to the increase in the crystallinity degree (crystal volume fraction) through a process of chemi-crystallization [13–18], which depends on dose and neutron flux level [19,20]. The increase in the volume fraction of crystallites and in their size was revealed by means of dynamic mechanical analysis (DMA, tan (ϕ) and elastic modulus measurements as a function of temperature). Besides, by increasing the irradiation dose the crystallinity degree is destroyed [19,20]. Indeed, neutron damage assessment appears as an important engineering consideration for the application of EPDM in the electrical industry, because the damage produced by long-term exposition of EPDM to electromagnetic fields [21] can be achieved by short neutron irradiation doses and/or times.

2. Experimental

2.1. Samples

Samples were commercial ethylene–propylene-diene-monomer (EPDM) used as housing of non-ceramic electrical insulators (Avator of Sitece Electrical Industries, Buenos Aires, Argentina) which are usually employed in outdoor transmission lines of 66 kV [21]. The nominal molar composition of the rubber was 55% ethylene – 42% propylene and 3% diene-monomer. The EPDM used in the present work was reinforced with ceramic particles in a proportion of 44 wt%, determined by means of pyrolysis. Ceramic was identified, by means of X-ray studies plus refining of the patterns, as Bayerite (alumina-trihydrate, ATH, Avator of Sitece Electrical Industries, Buenos Aires, Argentina) having a triclinic lattice with $a = 17.338$ Å, $b = 10.086$ Å, $c = 9.73$ Å, $\alpha = 94.17^{\circ}$, $\beta = 92.13^{\circ}$ and $\gamma = 90^{\circ}$ [19,20].

Samples of parallelepiped form of 9 mm width, 8 mm thick and 38 mm length were cut from the rubber with a low speed saw. Subsequently, the final size of the sample was adjusted by mechanical polishing in distilled water, in accordance to the requirements of each kind of test.

2.2. Neutron irradiation

Neutron irradiations were performed under different conditions in two different nuclear reactors, the RA-6 and the RA-4 of the National Atomic Energy Commission of Argentina, where the main differences were the flux level and power of operation. In both reactors the samples were irradiated at room temperature in air at atmospheric pressure.

Samples irradiated at the RA-6 nuclear reactor will be identified as samples under high flux irradiation. All samples were irradiated with bismuth and cadmium filters. The doses and fluxes related to neutron irradiation are written in Table 1.

In the RA-4 the samples were placed inside of a cylinder of polymethyl-methacrylate (PMMA) of 250 mm length and 25 mm diameter with a wall and bases of thickness 2 mm and 20 mm, respectively. Samples irradiated at the RA-4 nuclear reactor will be identified as samples under low flux irradiation, see Table 1 and Refs. [19,20,22] for more details.

The charge with Bayerite in the EPDM gave rise to an additional irradiation process through β particles, during and after the neutron irradiation. In all the irradiated samples the activity was smaller than 5.6×10^4 Bq. Considering the whole reactions of the neutron irradiation process over the Bayerite a β dose rate less than 3 Gy/h can be obtained for the irradiation at the RA-6 [20].

Table 1
Status of the studied samples, detailing the doses and neutron fluxes used during the neutron irradiation processes.

Sample denomination	Dose (Gy)	Thermal neutron flux (n/cm^2 s)	Fast neutron flux (n/cm^2 s)
A	0	0	0
High flux irradiation			
H	415	8.5×10^7	2.75×10^8
I	830	8.5×10^7	2.75×10^8
J	4150	1.7×10^8	5.5×10^8
K	8300	1.7×10^8	5.5×10^8
Low flux irradiation			
C	12.7	5.7×10^7	5.0×10^7
E	38.2	5.7×10^7	5.0×10^7
F	51.0	5.7×10^7	5.0×10^7

2.3. Measurements

Dielectric relaxation (DR) measurements were carried out in an automated measuring system using a Tektronix TDS-210 (USA) real-time Digital Sampling Oscilloscope, an Instek GW-830 (Taiwan) Synthesized Signal Generator and a Broadband Dielectric Interface designed and built at the Laboratory of Liquid Systems, Physics Dept., Faculty of Engineering, UBA, together with a signal processing algorithm based on the Fast Fourier Transform (FFT). All the measurement and signal processing software was developed at the Laboratory and uses the VEE™ (Version 3.0 or higher) graphical language environment of Agilent Corp. (USA) running on the Windows 98™ (or higher) operating system from Microsoft Corp. (USA). Further details on the dielectric measuring system are given in Ref. [23]. Samples were placed at a temperature of 294 K ± 1 K in a broadband coaxial cell. Dielectric measurements were made at 15 logarithmically spaced frequencies for each decade in the range between 15 Hz and 1500 KHz. In addition, measurements in a Topward 5100 (Taiwan) LCR Meter were made to check the results at the following frequencies: 100 Hz, 120 Hz, 400 Hz, 1 KHz, 5 KHz, 10 KHz and 15.7 KHz.

The lowest measurement frequency for Dielectric Relaxation measurements was 15 Hz since the small size of the samples precluded the use of guard electrode techniques. It must be remarked that guard electrode techniques are necessary at low frequencies to mitigate the effects of surface leakage currents on the sample. These currents originate large uncertainties in the measurement of dielectric losses at frequencies below a few tens of Hz [21]. Samples used in DR studies were taken from the same parallelepiped used for DMA studies. Rectangular plates (5 mm × 4 mm approximately) with a thickness of about 2 mm were used. The dimensions of each sample were measured with a Digimess 110 digital calliper made by Shinko Precision (China), to an accuracy of ±0.01 mm. Prior to measurements, the sample surfaces were carefully cleaned and rinsed in deionised water of low conductivity (>0.1 μS/cm), and then placed over filter paper in air at room temperature for 1 h. Deionised water was obtained in the laboratory from a water deionising system made by Silicon Química (Argentina). The conductivity of the water was measured, immediately before being used, with an "on-line" conductivity meter model HI 983304 made by Hanna Instruments (Portugal).

Measurements of dynamic mechanical analysis (DMA), loss tangent (tan (ϕ)) and elastic shear modulus (G') were carried out as a function of temperature at frequencies between 1 and 70 Hz, in a equipment developed at the Laboratory of Materials (CONICET-UNR), Rosario. The temperature range of the measurements was between 180 K and 370 K and the heating rate was of about 1 K/min. Measurements were performed under Argon atmosphere at atmospheric pressure. The samples for DMA studies were

parallelepiped bars of 5 mm width, 4 mm thick and 30 mm length. The maximum shear strain on the sample was 2×10^{-4}. Tan (ϕ) values were independent of the amplitude of the oscillating strain, i. e. doubling the applied stress led to the doubling of the strain response [24]. The estimated uncertainties for tan (ϕ) and G' were less than 3% and 10%, respectively. See Refs.[19,20] for more experimental details.

3. The model

We consider a two-phase polymer partitioned in different cubes which form a sizeable bulk material, in such a way that a given cube can be of one phase and its neighbourhood can be of the same phase or of the other one. Fig. 1a shows the representation for a two-phase polymer, which was used in a previous work for describing the dielectric response from dynamic mechanical analysis [12]. In fact, the smallest size of the partition must allow to describing the morphology of the partitioned material in such a way that permit us to obtain the best representation of this partition made in the material. As it was mentioned in the introduction section, a partition of a polymer made in this mode has some similarity to Takayanagi's model [1,10] used for describing oriented polymers.

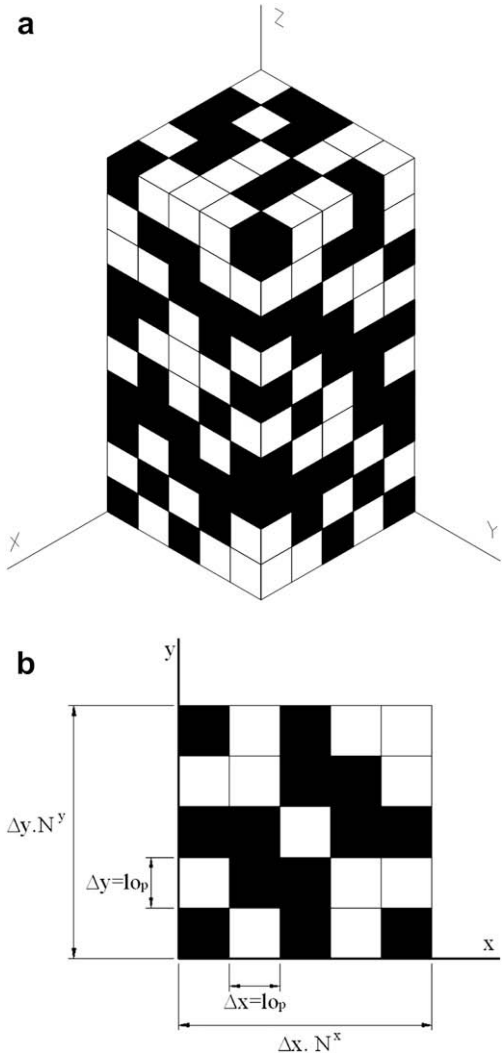

Fig. 1. a: Three-dimensional representation of the partition of a polymer sample. Taken from Ref. [12]. b: Representation of the base (at the $z = 0$ plane) of the polymer sample in Fig. 1a. Δx and Δy are the size of the partition over each axis and N^x and N^y are the number of partitions laying on the x- and y-axis respectively. Taken and adapted from Ref. [12].

In Fig. 1b, the base of the parallelepiped is showed at the $z = 0$ plane, where Δx and Δy are the size of the edge in the x- and y-axis, respectively; of the base of a single cube. In addition, considering that the distribution of inclusions is homogeneous in volume, it results that the number of partitions related to inclusions in each column along the z-axis, is approximately the same.

In the present work the crystalline zones in a two-phase polymer, will be considered as an inclusion embedded into a continuous and homogeneous matrix. The growing of crystalline zones in two-phase polymers, e.g. by chemi-crystallization; leads to a strain misfit into the matrix. An evaluation of the behaviour of the strain misfit during the development of the above mentioned processes can be done through the application of the here presented model. Even if the model is based on the partitioned material, where each part of the partition is in contact with each other, i.e. interaction effects are taking into account, the case of dilute inclusion can also be satisfied. In fact, a dilute case will be easily described by decreasing the volume fraction of the inclusions into the matrix. This point will be clarified after observing the mathematical treatment of the model.

The degree of strain misfit will be calculated considering the equilibrium condition in a homogeneous elastic continuous, which results after forcing to locate into a cubic hole of the matrix (with edge length lo_p) a cubic inclusion of larger size (edge length, $lo_p + \in lo_p$, with $0 \leq \in \leq 1$). Once the inclusion is located into the hole, stresses release, giving rise to a movement of the interface between the inclusion and the matrix. This idea for describing the degree of strain misfit into a matrix was reported earlier by Lee et al. [8] treating diluted spherical precipitates, without elastic interaction between the inclusions themselves located into the matrix. Besides, the treatment by Eshelby cited in Ref. [3] has also similarity to Lee et al.'s work.

It is convenient to point out at this time, that we have chosen Lee et al.'s basic ideas for developing our model, because Lee's model introduces a coefficient to measure the degree of misfitting. This coefficient makes easy to handle and to interpret the experimental results, in contrast to other models reported in the literature where the term related to the misfitting is hard to be handled and interpreted due to its mathematical complexity.

Fig. 2 shows a plane (z,y) of the partitioned sample at $x = v$, where the size of the partitioned matrix, Δx, Δy, Δz; was chosen equal to lo_p. The model for calculating the degree of the strain misfit starts with the following considerations:

a) The volume element located at (v,m,j) of the whole partitioned matrix (see Figs. 1 and 2), which is plotted by means of full fine lines in Fig. 2, is cut and removed out of the matrix; leading to a cubic hole of edge lo_p. In other words, a cubic volume is cut from the non-distortioned initial cubic lattice.
b) An inclusion of size $lo_p + \in lo_p$, with $0 \leq \in \leq 1$, plotted by means of broken lines will be firstly compressed to fit into the hole of the matrix and subsequently placed in.
c) The inclusion is mechanically released and then the boundaries of the hole, in the x-, y- and z-axis, displace to a position $lo_p + \beta \in lo_p$, with $0 \leq \beta \leq 1$, where the equilibrium of stresses is achieved. This state is represented by the wider lines in Fig. 2.

We consider the movement of each boundary in each axis as a plane front which moves until the equilibrium of stresses in each axis is reached. The contribution to the movement in the x-axis owing to the configuration of stresses in the y- and z-axis is obtained by the linear superposition principle through the Poisson ratio.

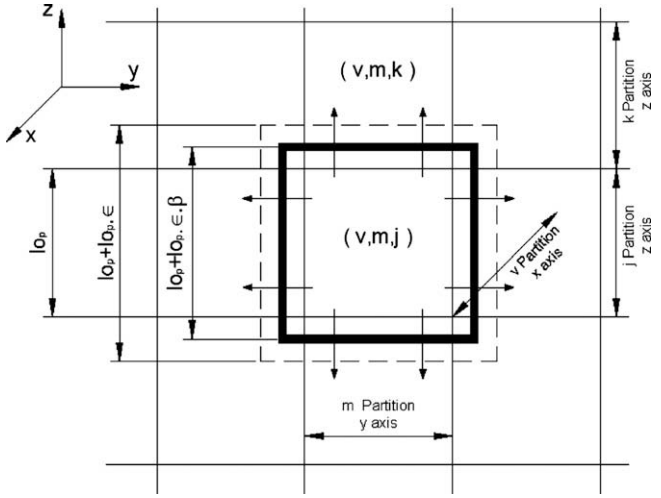

Fig. 2. Accommodation of the misfit strain by the appearance of an inclusion into the material matrix. Fine full line: Initial size of the base of the cube of the partitioned material. Broken line: Size of the inclusion free of stresses. Wider full line: Equilibrium position of the boundary between the inclusion and the matrix, after location of the inclusion into the matrix hole (see details in the text). Arrows in the figure indicate the pushing effect of the inclusion on the matrix.

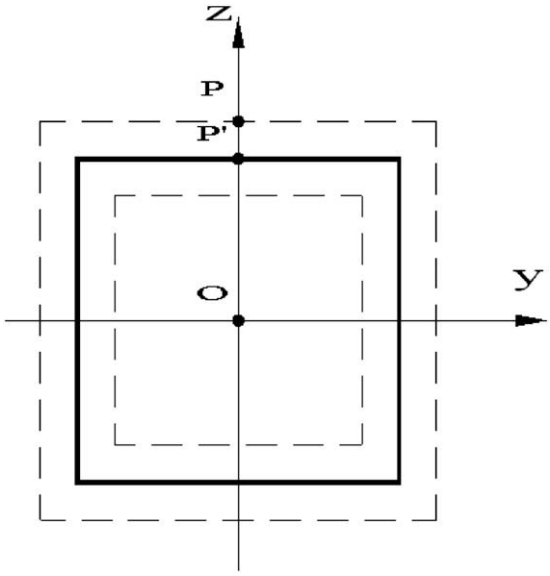

Fig. 3. Movement of the boundary of the inclusion (*v,m,j*) after location in the matrix hole and achievement of the mechanical equilibrium.

It is well know that the apexes of a cubic-shaped inclusion are points where stresses concentrate and in addition, different shapes of inclusion as plates or needles lead to different patterns of stresses into the matrix [3,5,6]. However, this representation based on cubic inclusions does not diminish the potentiality of the model, since we are looking for the bulk effect produced by the strain misfit in a mean field approximation. That is, the model does not look for the local effect due to the shape of the inclusion into the matrix. In fact, the non-uniform stress distribution of both, into the inclusion or into the matrix are averaged by the mean-field approximation, i.e. we are transforming the non-uniform stress distribution field in a homogeneous average stress.

To follow the crystallinity degree evolution in semi-crystalline rubbers as EPDM is very complicate, because the very low volume fraction of crystals in the matrix, which makes X-ray or differential thermal analysis (DTA) measurements almost unable to describe the cited evolution. However, it should be remarked that the model proposed in this work will be able to describe the experimental results concerning the evolution of crystalline phases in EPDM rubber.

3.1. The one-dimensional case

Let's start the analysis considering in the one-dimensional case, the movement of the boundary in the *z*-axis, produced by the inclusion located at (*v,m,j*) and its effects over the neighbour matrix element (*v,m,k*), see Fig. 2. The displacement of the boundary of the element (*v,m,j*) from the initial position (position P in Fig. 3) after the inclusion is forced into the hole and released mechanically achieving the mechanical equilibrium, leads to the movement of the P-point from the position P to P′, Fig. 3.

We consider, that the inclusion and the matrix are homogeneous media, and due to the symmetry of the problem the centre of the inclusion, O point, will not change its position during the deformation process and the achievement of the stresses equilibrium, Fig. 3. Then, as it is shown in Fig. 4, any point inside the inclusion between the initial state (original size, free of stresses) and after forcing the inclusion into matrix and subsequent achievement of the mechanical equilibrium, moves from $(z + z\in)$ to $(z + z\in\beta^z)$, where β^z means the misfit coefficient along the *z*-axis. This leads to a displacement in the *z*-axis, $u_i(z)$, that is

$$u_i(z) = (z + z\in) - (z + z\in\beta^z) \tag{1}$$

$$u_i(z) = z\in(1 - \beta^z) \tag{2}$$

Consequently the mean strain inside the inclusion (averaged by the mean field approximation) in the *z*-axis, ε_i^z, results,

$$\varepsilon_i^z = \frac{\partial u_i}{\partial z} = \in(1 - \beta^z) \tag{3}$$

Here after the magnitudes corresponding to the inclusion or to the matrix, will be noted with a subscript *i* or *m*; respectively. In addition, either the direction for the strain misfit coefficient, β, and for the number of inclusions or matrix elements (N) will be denoted through a supra-subscript.

Now, we will study the resulting mean strain inside the matrix element. Considering that there exists an inclusion concentration

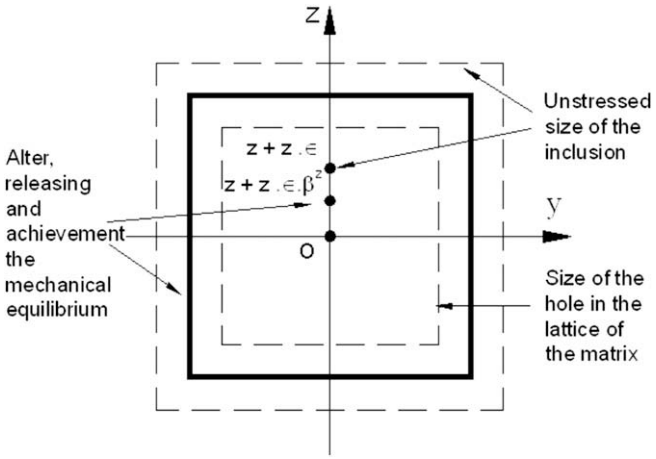

Fig. 4. Detail of the representation of Fig. 3, showing the displacements into the inclusion.

lying in the z-axis N_i^z/N_m^z (where N_i^z and N_m^z are the number of inclusions and the number of matrix elements, respectively, which satisfy the condition $N_i^z + N_m^z = N^z$), the N_i^z inclusions move the boundaries of the N_m^z partitions, in such a way that to the partition (v,m,k) corresponds the following displacement $z + z\in\beta^z N_i^z/N_m^z$, see Fig. 5.

Then, the displacement in the z-axis for the matrix elements can be written,

$$u_m(z) = z \in \beta^z \left(\frac{N_i^z}{N_m^z}\right) \tag{4}$$

Therefore, the strain inside the matrix element in the z-axis, ε_m^z, results,

$$\varepsilon_m^z = \frac{\partial u_m}{\partial z} = \in \beta^z \left(\frac{N_i^z}{N_m^z}\right) \tag{5}$$

By working Eq. (5) we obtain,

$$\varepsilon_m^z = \in \beta^z \left(\frac{N_i^z/N^z}{N_m^z/N^z}\right) \tag{6}$$

and defining in the usual mode the volume fraction both for the inclusions and for the matrix elements of the partioned material in the z-axis, such that

$$fr_i^z = N_i^z/N^z \tag{7}$$

$$fr_m^z = N_m^z/N^z \tag{8}$$

we can write

$$\varepsilon_m^z = \in \beta^z \left(\frac{fr_i^z}{fr_m^z}\right) \tag{9}$$

The mechanical equilibrium conditions at the boundary between the adjacent elements (v,m,j) and (v,m,k), according to the Reuss approximation [1,5] (see Fig. 2), implies

$$\sigma_i^z = \sigma_m^z \tag{10}$$

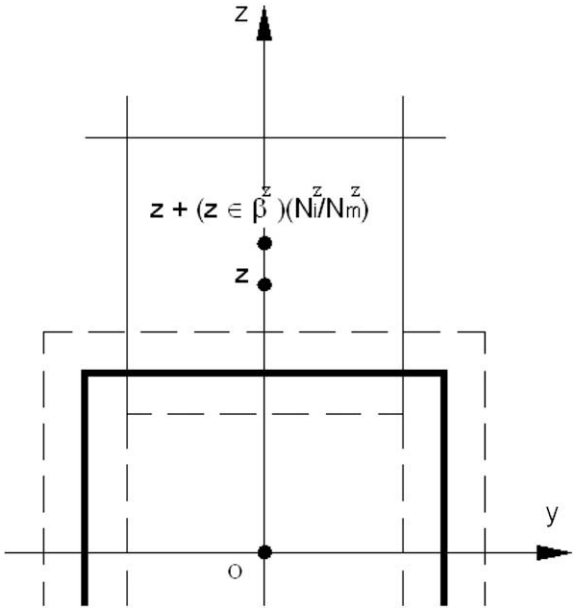

Fig. 5. Displacements into the matrix element produced by placing the inclusion in its hole.

Eq. (10), represents the mechanical equilibrium condition for a direction perpendicular to the surface of the interface between the amorphous and crystalline phases.

Applying Hooke's law and considering the Young moduli for the matrix and inclusion, E_i and E_m, respectively, we can obtain

$$\varepsilon_i^z E_i = \varepsilon_m^z E_m \tag{11}$$

$$\in (1-\beta^z) E_i = \in \beta^z \left(\frac{fr_i^z}{fr_m^z}\right) E_m \tag{12}$$

from where the misfitting coefficient in the z-axis, β^z, can be obtained as a function of the Young moduli and volume fraction of both inclusions and matrix,

$$\beta^z = \frac{1}{1 + \left(\frac{E_m}{E_i}\right)\left(\frac{fr_i^z}{fr_m^z}\right)} \tag{13}$$

If we consider that the material has a random distribution of inclusions in its bulk, the ratio between the volume fraction of the inclusions and the elements of the matrix in the three-axis directions is approximately the same, and then we can write

$$\left(\frac{fr_i^z}{fr_m^z}\right) = \left(\frac{fr_i^x}{fr_m^x}\right) = \left(\frac{fr_i^y}{fr_m^y}\right) = \left(\frac{fr_i}{fr_m}\right) \tag{14}$$

Consequently, from Eq. (13) as it could be expected, it results

$$\beta^z = \beta^x = \beta^y = \beta \tag{15}$$

Therefore, we have obtained the expression for the misfit of strain in one-dimensional representation, that is

$$\beta = \frac{1}{1 + \left(\frac{E_m}{E_i}\right)\left(\frac{fr_i}{fr_m}\right)} \tag{16}$$

3.2. The three-dimensional case

In the following paragraphs we will introduce the coupled strain effects in the three-dimensional network of the partitioned material of Fig. 1. In fact, the degree of displacement of the boundary in the z-axis in Fig. 2 for the inclusion, when the contribution of the neighbourhood in the x- and y-axis is taken into account leads to a reduction of the original displacement. Indeed, the compression stresses from the x- and y-axis, through the Poisson modulus produce a displacement in opposite direction to the produced during the achievement of the equilibrium of stresses in the one-dimensional study. Then, considering now the effects along the z-axis due to the inclusions lying in the y- and x-axis and using the linear superposition principle, the total strain in the z-axis for the inclusion element (v,m,j), $\varepsilon^z{}_{iT}$, can be written as

$$\varepsilon_{iT}^z = \varepsilon_i^z - \varepsilon_i^x \nu_i - \varepsilon_i^y \nu_i \tag{17}$$

where ν_i is the Poisson modulus of the inclusion partition, and ε_i^x and ε_i^y have the same meaning that ε_i^z for the one-dimensional treatment. Remembering that the strain inside the inclusion has the form given by Eq. (3), $(\varepsilon_i^z = \in(1-\beta^z))$, it results

$$\varepsilon_{iT}^z = \in (1-\beta^z) - \in (1-\beta^x)\nu_i - \in (1-\beta^y)\nu_i \tag{18}$$

From Eq. (15) we can re-write Eq. (18), with only one misfit coefficient, that is

$$\varepsilon_{iT}^{z} = \in(1-\beta)\,(1-2\nu_i) \tag{19}$$

A straightforward analysis, allows us to write the total strain in the three-dimensional case in the z-axis as a function of an average misfit coefficient for the whole volume of the material, β_b, such that

$$\varepsilon_{iT}^{z} = \in(1-\beta_b) \tag{20}$$

Therefore, relating Eqs. (19) and (20) and considering the interactions of the partitions in the x- and y-axis, we can write the resulting strain inside of a single inclusion (v,m,j) lying in the z-axis, ε_i^z of Eq. (3), as

$$\varepsilon_i^z = \frac{\in(1-\beta_b)}{(1-2\nu_i)} \tag{21}$$

The total strain in the adjacent matrix element (v,m,k) in the z-axis, considering also the interactions in the x- and y-axis, results

$$\varepsilon_{mT}^{z} = \varepsilon_m^z - \varepsilon_m^x\nu_m - \varepsilon_m^y\nu_m \tag{22}$$

Substituting the value of the strain in the matrix given by Eq. (9) in the above expression, we obtain

$$\varepsilon_{mT}^{z} = \in\beta^z\left(\frac{fr_i^z}{fr_m^z}\right) - \in\beta^x\left(\frac{fr_i^x}{fr_m^x}\right)\nu_m - \in\beta^y\left(\frac{fr_i^y}{fr_m^y}\right)\nu_m \tag{23}$$

Remembering that β and the ratio between the volume fraction of inclusions and matrix elements in the three-axis is the same, it results

$$\varepsilon_{mT}^{z} = \in\beta\left(\frac{fr_i}{fr_m}\right)(1-2\nu_m) \tag{24}$$

A similar treatment to the one made for the inclusion, allows us to write the total strain in the three-dimensional case in the z-axis for the whole volume of the material as a function of an average misfit coefficient, β_b, such that

$$\varepsilon_{mT}^{z} = \in\beta_b\left(\frac{fr_i}{fr_m}\right) \tag{25}$$

Then from Eqs. (24) and (25) and using Eq. (9) the resulting strain in a single matrix element (v,m,k) can be calculated as

$$\varepsilon_m^z = \frac{\in\beta_b\left(\frac{fr_i}{fr_m}\right)}{(1-2\nu_m)} \tag{26}$$

Once the equilibrium is reached at the boundary between the inclusion (v,m,j) and the matrix (v,m,k), we can write

$$\varepsilon_i^z E_i = \varepsilon_m^z E_m \tag{27}$$

Substituting in the above equation the results from Eq. (21) and (26), it results

$$\frac{\in(1-\beta_b)}{(1-2\nu_i)}E_i = \frac{\in\beta_b\left(\frac{fr_i}{fr_m}\right)}{(1-2\nu_m)}E_m \tag{28}$$

and working the Eq. (28), we have

$$(1-\beta_b)E_i = \beta_b\left(\frac{fr_i}{fr_m}\right)\frac{(1-2\nu_i)}{(1-2\nu_m)}E_m \tag{29}$$

from where β_b can be easily obtained, that is

$$\beta_b = \frac{1}{1+\left(\frac{E_m}{E_i}\right)\left(\frac{fr_i}{1-fr_i}\right)\frac{(1-2\nu_i)}{(1-2\nu_m)}} \tag{30}$$

From Eq. (30) we can conclude that when $fr_i \to 0$ then, $\beta_b \to 1$ which implies that the misfit of strain in the matrix will be negligible, as it should be.

4. Comparison of the present results with the results of the Lee et al. earlier model

Lee et al. [8], for the misfit coefficient around a spherical precipitate considered as an inclusion, β_l, found the following equation

$$\beta_l = \frac{\alpha\,\gamma}{\alpha(\gamma-1)+1} \tag{31}$$

where α=$(1+\nu_m)/3(1-\nu_m)$, γ=$\mu_i(1+\nu_i)(1-2\nu_m)/\mu_m(1+\nu_m)(1-2\nu_i)$, μ is the shear modulus and ν is the Poisson modulus. The subscripts i and m refer to the inclusion and matrix values, respectively.

By working, we have

$$\beta_l = \frac{1}{1+\frac{\mu_m}{\mu_i}2\frac{(1-2\nu_i)}{(1+\nu_i)}} = \frac{1}{1+\frac{E_m}{E_i}2\frac{(1-2\nu_i)}{(1+\nu_m)}} \tag{32}$$

where E is the Young modulus.

On the other hand, re-writing Eq. (30) in the following form

$$\beta_b = \frac{1}{1+\left(\frac{E_m}{E_i}\right)\left(\frac{fr_i}{1-fr_i}\right)\frac{(1+\nu_m)}{(1-2\nu_m)}\frac{(1-2\nu_i)}{(1+\nu_m)}} \tag{33}$$

and comparing with the Eq. (32) we can observe the differences between the predicted β coefficients by the both models.

The present model is related to the mean strain inside the whole matrix. In comparison to Lee's model, which takes into account only one inclusion in the matrix, the proposed model is a more general one, which allows for interaction between inclusions, and so, for different amount of inclusions fractions within the matrix. In that sense β_b, which corresponds to a misfit coefficient, has to be considered as a measurement of the average inclusion strain caused by the matrix or vice versa.

5. Application to the neutron irradiated EPDM

As said before, we reported that neutron irradiation on ethylene–propylene-diene M-class rubber (EPDM) leads to the increase in the crystallinity degree (crystal volume fraction) of this two-phase polymer through a process of chemi-crystallization [13–18], which depends on dose and neutron flux level [19,20]. The increase in the volume fraction of crystallites and in their size was revealed by means of DMA response. The crystals in EPDM can be considered as inclusions into the rubber matrix that strengthen it, but the behaviour of the elastic modulus does not always reveal the effect of the crystalline degree development. Indeed, many times the hardening of the matrix cannot be detected due to the simultaneous occurrence of chain scission and chemi-crystallization processes in the rubber during irradiation, which lead to a decrease in the elastic response of the matrix [19,20]. The contribution to the elastic modulus due to crosslinking promoted by the H-pull during the irradiation process is not taken into account, because the swelling studies did not reveal the appearance of the development of crosslinking points [19,20]. However, we cannot fully reject that some additional points of crosslinking may be developed during irradiation.

In the other hand, it has been already reported that the change in the crystallinity degree promoted by chemi-crystallization process in EPDM is difficult to be observed by means of other

experimental techniques, like X-ray diffraction or DTA [15,19,20]. DTA measurements allow to determine the appearance of the endothermic peak related to the melting of crystals at around 310 K, however it is still difficult to determine accurately the changes in the crystallinity degree from DTA measurements.

In this article we will show that the coefficient β of the previously presented model, gives an accurate measurement of the average strain into the matrix caused by both the appearance or growing of inclusions into a two-phase polymer as EPDM. Moreover, by comparing the DMA results and the evolution of the values of the coefficient β with the DR results, we will conclude that the relaxation time measured from the electrical excitation of the crystals caused by the dipoles in the amorphous zone is clearly related to both, the evolution of the crystallinity and the degree of internal stresses into the rubber matrix. We will present first the DMA results and we will compare then with both, the calculated values for the coefficient β and the DR measurements.

The effect of high flux irradiation, at a dose up to 415 Gy in EPDM samples, leads to a decrease in the crystallinity degree (crystalline volume fraction). This is revealed through the decrease in the intensity of the tan (ϕ) maximum which is related to the melting of the crystalline zones in the EPDM, as it was previously reported in Ref. [20], see Fig. 6. However, by increasing the irradiation dose a subsequent increase in the crystallinity degree is achieved. Indeed, Fig. 6 shows that the maximum of tan (ϕ) increases as irradiation dose increases for values higher than 415 Gy. In addition, crystals developed at irradiation doses higher than 415 Gy are larger than the ones appearing in the rubber matrix prior to irradiation. In fact, for dose higher than 415 Gy the temperature of the tan (ϕ) maximum (Tp) increases, indicating an increase in the size of the crystals, see right axis in Fig. 6.

In contrast, samples irradiated at low fluxes exhibited an increase in the volume fraction of crystals with respect to the initial volume fraction of the unirradiated ones, but the size of the crystals does not changed appreciably, as it was the case of irradiated samples at high flux. The maximum amount of crystals (volume fraction) for irradiated samples at low flux was achieved at around 32 Gy, see Fig. 7 [19,20].

In this work we have obtained the change in the crystallinity degree in EPDM by means of DR measurements performed in the same samples where DMA studies were realized. Fig. 8 shows the behaviour of the real part of the electric permittivity, ε', as a function of the frequency; for the high flux irradiated and unirradiated

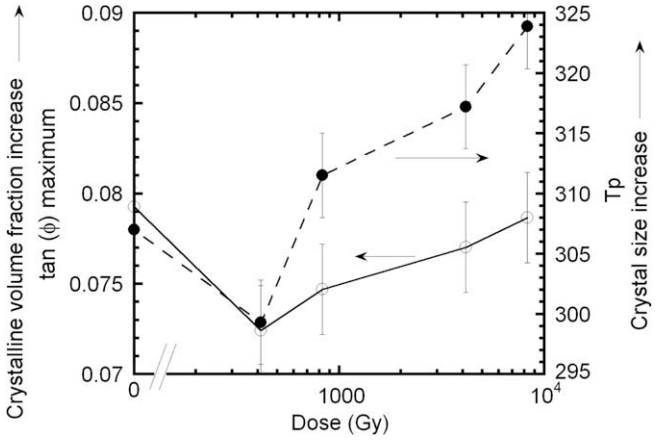

Fig. 6. Left axis: Maximum value of the tan (ϕ) measured in DMA as a function of the irradiation dose at high flux. An increase in the tan (ϕ) corresponds to an increase in the crystalline volume fraction, see text. Right axis: Temperature corresponding to the tan (ϕ) maximum as a function of the irradiation dose. An increase in Tp corresponds to an increase in the crystal size.

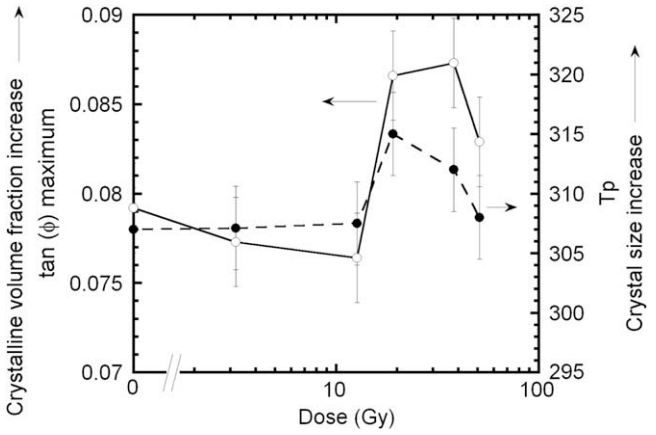

Fig. 7. Maximum value of the tan (ϕ) measured in DMA and the temperature corresponding to the tan (ϕ) maximum, as a function of the irradiation dose at low flux. Crystalline volume fraction and crystals size are related as indicated in Fig. 6.

samples detailed in Table 1. Fig. 9 is equivalent to Fig. 8, for low flux irradiated and for the unirradiated samples detailed in Table 1. Experimental data were fitted to a Cole–Cole equation, which correspond to a Havriliak–Negami equation with the parameter controlling the asymmetrical broadening equal to 1 [25–29]. Fitted curves are plotted by means of lines.

Table 2 summarises for the samples of Table 1 the results of the relaxation time, τ_0, obtained for fitting a Cole–Cole function to the measured data.

Fig. 10 shows the variation of the relaxation time, τ_0, as a function of the irradiation dose for high fluxes. The values of the misfit coefficient β which are also shown in Fig. 10, have been calculated using Eq. (16). We have utilized this equation due to the experimental limitation for obtaining, for the used samples, the values of the Poisson moduli which appear in the general Eq. (30). Nevertheless, using the one-dimensional approximation will not modify appreciably the analysis made in this work. In fact, unless a large change in the mechanical properties of the crystalline/amorphous

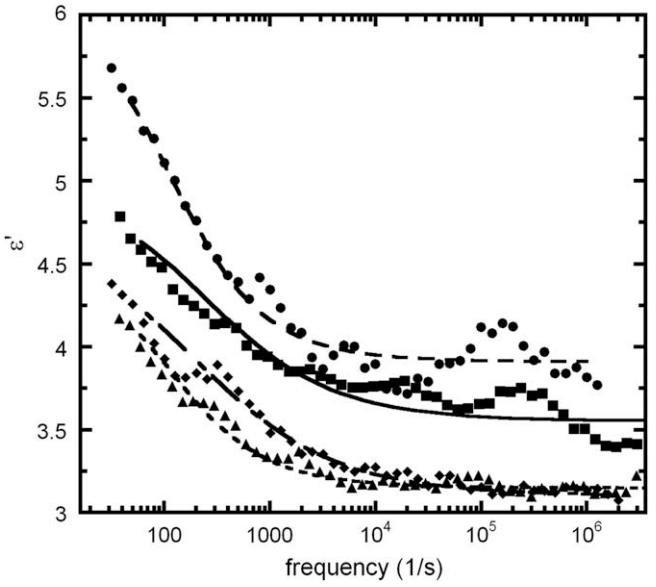

Fig. 8. Real part of the electrical permittivity as a function of frequency for non-irradiated and high flux irradiated samples. Non-irradiated: squares, circles: 415 Gy, diamonds: 830 Gy, triangles: 8300 Gy.

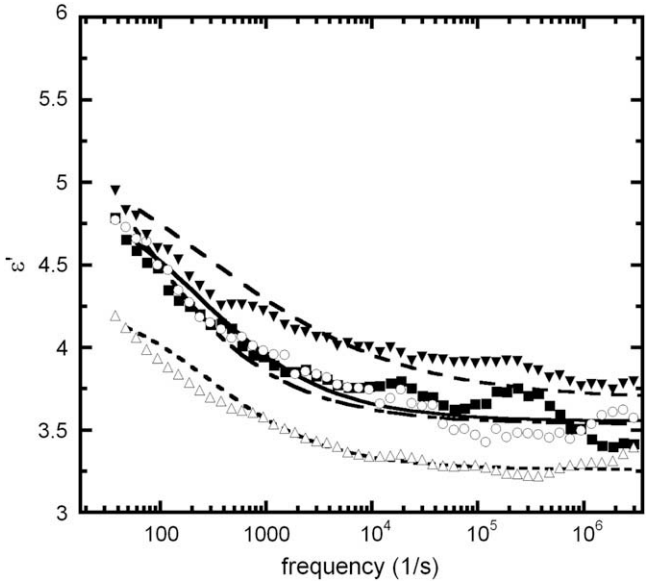

Fig. 9. Real part of the electrical permittivity as a function of frequency for non-irradiated and low flux irradiated samples. Non-irradiated: squares, empty circles: 12.7 Gy, empty triangles: 38.2 Gy, inverted triangles: 51 Gy.

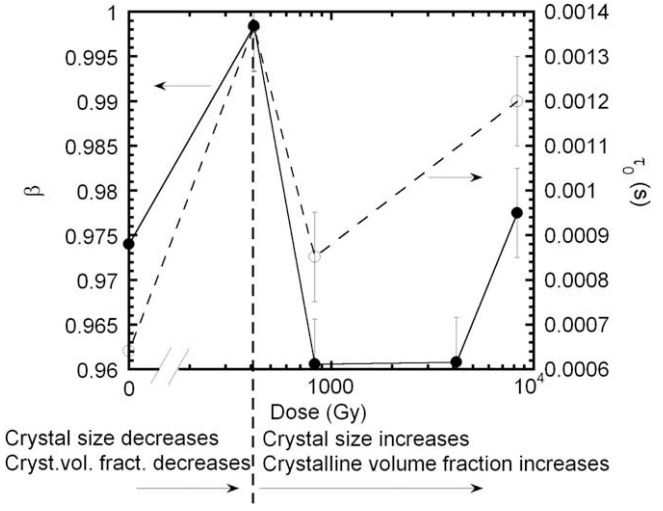

Fig. 10. Misfit coefficient β calculated through the new model using Eq. (16) (full circles) and relaxation time (empty circles) obtained from dielectric measurements as a function of the irradiation dose at high flux. Vertical broken line indicates the dose (415 Gy) where the crystalline volume fraction and the crystal size have decreased from the non-irradiated state, being the smallest values achieved, respectively. At higher doses than 415 Gy, the crystalline volume fraction and crystal size increase.

phases occurs, Poisson moduli ratio is constant. Then Eq. (16) obtained for the one-dimensional approximation differs only in a constant from Eq. (30). Therefore, Eqs. (16) and (30) show identical trends with crystalline/amorphous fractions; they differ only in the numerical value. In order to illustrate in a numerical manner the behaviour of β in neutron irradiated EPDM we will use Eq. (16), taking into account that its absolute value is not meaningful, only relative changes are.

The calculus of β requires the values of the Young moduli for the amorphous and crystalline phases E_m, and E_i respectively and their corresponding volume fractions fr_m and fr_i. Volume fractions have been obtained from the DMA measurements previously reported, in Refs [19,20]. Nevertheless, in Eq. (16) we have used the dynamic elastic shear modulus, G', instead of the Young modulus. The oscillating frequency in DMA tests from which we have calculated G', for all the tested samples, was close to 4 Hz. This frequency is inside the usual frequency range for polymer DMA tests. Other frequencies for performing the measurements can be chosen meanwhile, the approximations made in the calculations hold as valid. Anyway, this will not diminish nor obstruct the subsequent analysis made here. Mocellini et al. in a previously reported work [12] described the procedure for obtaining the values of G'_m and G'_i. This procedure is summarised in Appendix A.

Returning to Fig. 10, the initial state of the rubber exhibits a coefficient β with a value close to 0.975. Subsequently, for a dose of 415 Gy, where both the crystal size and volume fraction of crystals decrease (see Fig. 6), β goes close to 1, indicating that the accommodation of the strain misfit produced by the crystal inclusions causes practically negligible stresses into the matrix.

Increasing the dose, both the crystal size and the volume fraction increase, due to the chemi-crystallization promoted by the neutron irradiation; Fig. 6. Here the calculated values of β decrease, points for 830 Gy and 4150 Gy in Fig. 10. This is because the increase in size of the crystal inclusions and their volume fraction promote the appearance of new mechanical stresses into the matrix.

It should be noticed that, the relaxation time measured from the electrical excitation of the crystals caused by the dipoles in the amorphous zone reveals the behaviour of the crystallinity into the rubber matrix, as a function of the irradiation dose. In fact, the relaxation time increases with the deterioration of the degree of crystallinity at 415 Gy. Subsequently, the restoration of the crystallinity leads to a decrease in the relaxation time at 830 Gy. A zone with higher symmetry exhibits a higher rate of mobility and consequently a smaller relaxation time [27,28]. The development of

Table 2
Relaxation time obtained from fitting a Cole–Cole equation to the DR measurements.

Dosis (Gy)	Irradiation condition (low/high flux)	$(\tau_0 \pm 0.1) \times 10^3$ (s)
0-non-irradiated		0.6
12.7	Low	3.1
38.2	Low	0.5
51	Low	0.6
415	High	1.4
830	High	0.9
8300	High	1.2

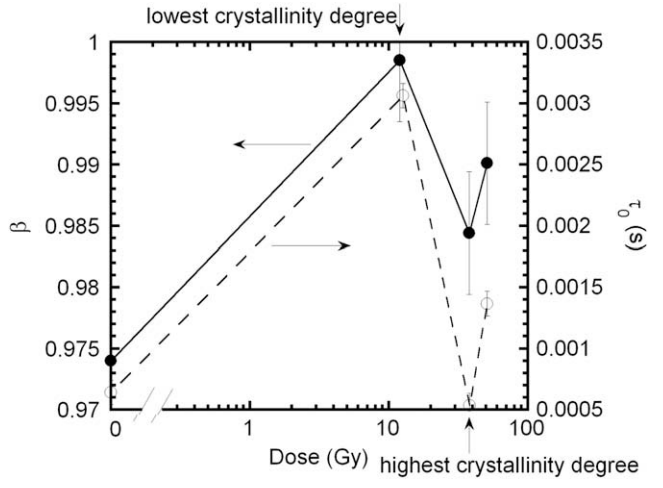

Fig. 11. Misfit coefficient β calculated through the new model using Eq. (16) and relaxation time obtained from dielectric measurements as a function of the irradiation dose at low flux. The irradiation doses for the highest and lowest degree of crystallinity achieved during the irradiation are indicated by means of arrows.

crystallinity in the samples by irradiation, that is, the increase of both volume fraction and size of crystals, leads to the increase of the internal stresses by the appearance of inclusions into the matrix (β decreases). At the same time, since these inclusions have a higher symmetry, the mobility under electrical excitation is larger and consequently the relaxation time is smaller. Therefore, the behaviour of the relaxation time results in agreement with the behaviour above exposed for the coefficient β. For irradiation at 8300 Gy, both β and the relaxation time have increased due to the deterioration of the rubber matrix as a consequence of the irradiation process, see Ref. [20].

For the low flux irradiated samples, we have performed dielectric measurements, Fig. 9, for samples in the states with the lowest and highest volume fraction of crystals, i.e. 12.7 Gy and 38.2 Gy, and also for the last dose achieved, 51 Gy (see Fig. 7). Fig. 11 shows the behaviour of β and the relaxation time as a function of the irradiation dose for low flux irradiated samples. At 12.7 Gy the deterioration of the initial crystallinity of the rubber in the as-received state occurs (see Fig. 7), and then $\beta \to 1$. The largest degree of crystallinity developed by chemi-crystallization, at 38.2 Gy, leads to a decrease in β, indicating that internal stresses are produced into the rubber, Fig. 11.

The behaviour of the relaxation time τ_0, shows a strong increase in the state of less crystallinity and a subsequent decrease after the development of the crystals by chemi-crystallization, in agreement with the above exposed about the correlation between the behaviours of the coefficient β and the relaxation time as a function of the degree of crystallinity. It should be pointed out that, in the case of low flux irradiated samples the behaviour of both the coefficient β and the relaxation time is related mainly to the volume fraction. That means that the change in the size of the crystals is smaller than for the case of high flux irradiated samples, see Figs. 6 and 7.

6. Conclusions

The present work presents a model, which evaluates the mean strain inside a material matrix with inclusions. In comparison to Lee's model, which takes into account inclusions without interaction in the matrix, the proposed model is a more general one, which allows for interaction between inclusions, and so, for different amount of volume fractions of inclusions within the matrix. In that sense the coefficient β measures the average inclusion strain in the whole matrix and vice versa.

Results show that the coefficient β of the presented model gives an accurate representation of the average strain in the rubber matrix caused by the crystallites in a two-phase polymer as EPDM. The coefficient β is closely related to the degree of crystallinity into the polymer and following the evolution of the values of this coefficient we can monitor the change in the crystalline degree into the rubber matrix.

Dielectric relaxation measurements were suitable for observing the changes in the crystallinity degree in EPDM and the results of the relaxation time obtained from these measurements are in agreement with both the different stages of crystallinity and the degree of internal stresses into the rubber matrix.

Acknowledgements

This work was partially supported by the Collaboration Agreement between the Universidad del País Vasco and the Universidad Nacional de Rosario Res. CS.788/88 – 1792/2003, UPV224.310-14553/02, Res. 3469/2007 and the new one signed Res. pending 2008, the CONICET-PIP No. 11220080102098 and 5665 and the PID-UNR (ING 115) 2005-2007 and (ING 227) 2008-2009.

Appendix A

The procedure for obtaining the quantities involved in the calculus of β will be described briefly here. At temperatures higher than the maximum in tan (ϕ), it is reasonable to consider that the contribution to the measured value in tan (ϕ) is originated from the amorphous phase instead of the semi-crystalline one. In addition, it is known that the dependence of the elastic modulus on temperature in a restricted range, like the studied in the present work, can be described by a linear approximation as in the text [12]. Therefore, by extrapolating linearly the curve from the high temperature part of the DMA spectrum for G' towards room temperature, we can obtain the value of G' corresponding principally to the amorphous phase at RT, G'_a (RT), since most of crystals have been melted. That is,

$$G'_a(RT) = G'_{a0} - m_k\, RT \tag{34}$$

where G'_{a0} is the ordinate at the origin, m_k is the slope of the linear extrapolation and RT is the room temperature in Kelvin. The temperature range for fitting the straight-line was determined from the linear zone of the corresponding tan (ϕ) curve, between the values at highest temperature and at 325 K. This temperature was chosen since it corresponds to the point where starts the split between the measured tan (ϕ) and the fitted tan (ϕ), from the highest temperature curves; see for more details Ref. [12]. In addition, following the Mocellini model [12], the volume fraction (frc) and elastic modulus (G'_c) of the crystalline phase can be calculated as follows,

$$frc \cong \frac{(G' - G'_a)}{G'_a} \tag{35}$$

where the volume fraction of the crystalline and amorphous phase satisfies the condition $frc + fra = 1$.

The elastic modulus corresponding to the crystalline phase can be obtained from

$$G'_c = \frac{frc\, G'\, G'_a}{G'_a - G'(1 - frc)} \tag{36}$$

Now with the values above, wee can obtain β from Eq. (16).

References

[1] Ward IM. Mechanical properties of solid polymers. 2nd ed. New York: John Wiley & Sons; 1990.
[2] Gauthier MW, editor. Engineered materials handbook. Ohio: ASM International; 1995.
[3] Eshelby JD. Proc R Soc London A 1957;241(20):376–96.
[4] Mori T, Wakashima K. Successive iteration method in the evaluation of average fields in elastically inhomogeneous materials. In: Weng GJ, Taya M, Abé H, editors. Micromechanics and inhomogeneity. The Toshio Mura 65th anniversary volume. New York: Springer-Verlag; 1990. p. 269–82.
[5] Mura T. Micromechanics of defects in solids. New York: Martinus Nijhoff Publishers; 1987.
[6] Kato M, Fujii T, Onaka S. Mater Sci Eng A 1996;211(1–2):95–103.
[7] Brinson LC, Knauss WG. J Appl Mech, ASM 1992;59(4):730–7.
[8] Lee JK, Earmme YY, Aaronson HI, Russell K. Metall Trans A 1980;11(A): 1837–47.
[9] Mori T, Tanaka K. Acta Metall 1973;21(5):571–4.
[10] Takayanagi M, Imada K, Kajiyama K. J Polym Sci C 1966;15:263–81.
[11] Mocellini RR, Zelada-Lambri GI, Lambri OA, Matteo CL, Sorichetti PA. IEEE Trans on Dielec and Elec Ins 2006;13(6):1358–70.
[12] Mocellini RR, Lambri OA, Matteo CL, Sorichetti PA. IEEE Trans on Dielec and Elect Ins 2008;15(4):982–93.
[13] Charlesby A. Atomic radiation and polymers. Oxford: Pergamon Press; 1960.
[14] Charlesby A, Callaghan L. Phys Chem Solids 1958;4:306–14.
[15] Davenas J, Stevenson I, Celette N, Vigier G, David L. Nucl Instrum Methods B 2003;208:461–5.
[16] Barker R, Sullivan A, Wise R. Testing rubber during processing and vulcanization. In: Baranwal KC, Stephens HL, editors. Basic elastomer technology. Akron: Rubber Division, ACS; 2001.

[17] Hofmann W. Rubber technology handbook. Cincinnati: Hanser Gardner Publications; 1989.
[18] Kramer O, Hvidt S, Ferry J. Dynamic mechanical properties. In: Mark J, Erman B, Eirich FR, editors. Science and technology of rubber. San Diego: Academic Press; 1994.
[19] Salvatierra LM, Lambri OA, Matteo CL, Sorichetti PA, Celauro CA, Bolmaro RE. Nucl Instrum Methods B 2004;225:297–304.
[20] Lambri OA, Salvatierra LM, Sánchez FA, Matteo CL, Sorichetti PA, Celauro CA. Nucl Instrum Methods Phys Res, B 2005;237:550–62.
[21] Sorichetti PA, Matteo CL, Lambri OA, Manguzzi GC, Salvatierra LM, Herrero O. IEEE Trans on Dielec and Elec Ins 2007;14(5):1170–82.
[22] Zelada-Lambri GI, Lambri OA, Bozzano PB, García JA, Celauro CA. J Nucl Mater 2008;380(1–3):111–9.
[23] Sorichetti PA, Matteo CL. Measurement 2007;40(4):437–49.
[24] Lambri OA. A review on the problem of measuring non-linear damping and the obtainment of intrinsic damping. In: Walgraef D, Martínez-Mardones J, Wörner CH, editors. Materials instabilities. New Jersey: World Scientific Publishing Co. Pvt. Ltd.; 2000. p. 249–80.
[25] Havriliak S, Negami S. J Polym Sci C 1966;14(B):99–117.
[26] Havriliak S, Negami S. Polymer 1967;8:161–210.
[27] Pendleton W. Electrical insulation, solids. In: Bever MB, editor. Encyclopedia of materials science and engineering, vol. 2. Oxford: Pergamon Press; 1986.
[28] Runt JP, Fitzgerald JJ. Dielectric spectroscopy of polymeric materials, fundamentals and applications. Washington, DC: American Chemical Society; 1997.
[29] Matteo CL, Lambri OA, Zelada-Lambri GI, Sorichetti PA, García JA. J Nucl Mater 2008;377(2):370–7.